

Protein resource allocation across subcellular compartments revealed by large-scale absolute quantitative proteomics in yeast

Downloaded from: https://research.chalmers.se, 2026-11-08 10:45 UTC

Citation for the original published paper (version of record):

Lu, H., Zhang, Z., He, S. et al (2026). Protein resource allocation across subcellular compartments revealed by large-scale absolute
quantitative proteomics in yeast. Proceedings of the National Academy of Sciences of the United States of America, 123(44): e2621208123-. http://dx.doi.org/10.1073/pnas.2621208123

N.B. When citing this work, cite the original published paper.

research.chalmers.se offers the possibility of retrieving research publications produced at Chalmers University of Technology. It covers all kind of research output: articles, dissertations, conference papers, reports etc. since 2004. research.chalmers.se is administrated and maintained by Chalmers Library

(article starts on next page)

PNAS RESEARCH ARTICLE | BIOPHYSICS AND COMPUTATIONAL BIOLOGY OPEN ACCESS

Protein resource allocation across subcellular compartments revealed by large-scale absolute quantitative proteomics in yeast

Hongzhong Lu[a,1], Zhendong Zhang[a], Siwei He[a], Yucan Zhang[b], Yuguang Wang[b,c], Fei Tao[a], and Jens Nielsen[d,e,1]

Affiliations are included on p. 9.

Contributed by Jens Nielsen; received June 15, 2026; accepted September 28, 2026; reviewed by Duccio Cavalieri and John P. Morrissey

Subcellular compartmentalization within complex membrane-bound organelles is a hallmark of eukaryal life, enabling metabolic specialization through spatial segregation. Here, we compiled a dataset encompassing 300 absolute quantitative proteomes, the largest to date, across two yeast species under diverse experimental conditions. Leveraging big data analysis, formula fitting, and machine learning, quantitative correlations among protein abundance, resource allocation, and cellular phenotypes were elucidated at a system level. We found that subcellular resource distribution is highly uneven and covaries with specific growth rate. Specifically, at high specific growth rates, the protein mass fraction (PMF) from certain compartments, (e.g., nucleus) is consistently reduced, coinciding with the increasing protein resource demand from ribosomes. Meanwhile, nutrient limitation may induce resource recycling by upregulating protein resources within specific compartments (e.g., vacuole) to sustain stress adaptation. Importantly, our integrative analysis indicates that PMF from a few subcellular compartments (e.g., nucleus and ribosomes) can accurately predict yeast physiological parameters (e.g., specific growth rate, oxygen uptake rate), and a limited protein set (≥ 23) could be used to capture the variation in resource allocation across seven major subcellular compartments. Furthermore, our comparative analysis between Crabtree-positive and Crabtree-negative species across conditions illustrates that subcellular resource allocation could be shaped by multiple factors and the two species differ markedly in their robustness to environmental perturbations. In summary, the high-quality quantitative proteomic dataset for yeast species offers an unprecedented opportunity for understanding the general principles underlying subcellular resource allocation, laying foundations for precision engineering of cell factories in synthetic biology.

resource allocation | organelle-scale | absolute proteomics | yeast species

Significance

Allocation of limited protein resources among specialized subcellular compartments is a cornerstone of eukaryal evolution and fitness. This study provides a systematic investigation of protein resource allocation at the subcellular level across diverse environmental conditions in two yeast species. Thorough analysis of this unified, absolute quantitative proteome atlas revealed that yeast cells dynamically redistribute resources among distinct compartments to optimize fitness. We demonstrate that protein resource allocation is tightly coupled to specific growth rate and nutrient availability, governed by sophisticated trade-offs among subcellular compartments. Notably, meta-analysis of these proteome data uncovered quantitative correlations among individual protein abundances, subcellular resource distribution, and key growth phenotypes. This comprehensive dataset will empower broader studies of subcellular organization and systems-level metabolism.

The evolutionary origin of eukaryal cells, driven by endosymbiosis between an archaeal host and bacterial ancestors, gave rise to the elaboration of complex membrane-bound organelles and subcellular compartments (1). Compartmentalization allows cells to optimize resource utilization, mitigate biochemical incompatibilities, and improve the catalytic efficiency of enzymes through the spatial proximity effect (2). In particular, key compartments, such as mitochondria, peroxisomes, and the nucleus, play central roles in diverse metabolic activities, such as energy production, redox balance, genetic regulation, protein synthesis, and degradation. The division of labor and interorganellar crosstalk not only sustain fundamental cellular processes but also establish a hierarchically organized metabolic network, forming the foundation for advanced biological functions. However, despite their central role in eukaryal physiology and growing significance for metabolic engineering (3), fundamental principles governing how cells allocate protein resources among subcellular compartments are still not well understood.

Recent advances in quantitative proteome analysis based on mass spectrometry (4) have pioneered systems biology studies of *Saccharomyces cerevisiae*, a key model for eukaryal biology. Quantitative proteome analysis has enabled profiling the dynamic changes of protein abundance in yeast under varying conditions, e.g., nutrient limitation (5, 6), growth phase shifting (7), gene perturbation (8), and cell cycle switching (9, 10). The subsequent comparative analysis of proteomics between distinct conditions helps to illustrate how cell metabolism is tuned to adapt to various perturbations (11). It clearly shows that the abundances of some enzymes increase linearly with specific growth rate (12), the so-called growth laws. It is also found that the synthesis of enzymes in some compartments or pathways is more than needed, which is related to protein resource preallocation for more flexible adaptation under fluctuating conditions (13, 14). Moreover, the comparative proteomic analysis between Crabtree-positive and Crabtree-negative yeast species displayed that the two types of species are significantly different in efficiency of translation and

Reviewers: D.C., Universita degli Studi di Firenze; and J.P.M., University College Cork.

The authors declare no competing interest.

Copyright © 2026 the Author(s). Published by PNAS. This open access article is distributed under Creative Commons Attribution-NonCommercial-NoDerivatives License 4.0 (CC BY-NC-ND).

[1]To whom correspondence may be addressed. Email: hongzhonglu@sjtu.edu.cn or JNI@bii.dk.

This article contains supporting information online at https://www.pnas.org/lookup/suppl/doi:10.1073/pnas.2621208123/-/DCSupplemental.

Published October 27, 2026.

Downloaded from https://www.pnas.org by 155.4.17.34 on November 6, 2026 from IP address 155.4.17.34.

energy generation (15, 16). Integrating proteomics with genomics and transcriptomics also provides valuable insights into how genetic and transcriptional regulation influences protein abundances (17). Thus, proteome analysis facilitates the in-depth studies of yeast metabolism with high resolution.

Protein localization always reflects the protein's unique function in cellular metabolism as a result of evolution. Due to the importance of protein locations, various procedures have been developed to map the protein onto specific locations within the cell (18–22). Meanwhile, the progresses in absolute quantitative proteomic analysis provide unique chances to explore how resource allocation at the compartment level determines cell metabolic rewiring. As an example, mitochondrial proteome analysis by Bartolomeo et al. (7) quantified the cellular metabolic adaptive responses during diauxic shift, showcasing the protein resource reallocation from the cytosol to the mitochondria when growth switches from fermentative to respiratory metabolism. Proteome analysis at the subcellular level also enables the setting of new constraints for the metabolic model for the better simulation of cellular behavior. For example, the mitochondrial protein mass fraction (PMF) calculated by absolute proteomics could be used to constrain metabolic models to simulate the Crabtree effect in yeast at high specific growth rates (23). However, the current proteome analysis at a subcellular level only focuses on several intensively studied compartments, e.g., mitochondria, and the protein resource allocation at other major compartments (or subcompartment) was never investigated systematically across different yeast species under various growth conditions.

To address the above issues, we here reconstructed the largest standardized atlas of absolute quantitative proteomes for yeast, encompassing 300 datasets spanning two yeast species—*S. cerevisiae* and *Issatchenkia orientalis*. We integrated disparate proteomic datasets from chemostats, batch cultures, and stress conditions into a unified large-scale dataset, enabling cross-condition meta-analysis. Further, the protein resource allocation at a subcellular level was thoroughly explored under different specific growth rates, stressful conditions, and yeast species to reveal the design principles of living systems. With the large-scale proteomic dataset, the precise quantitative links among protein abundance, resource distribution, and cellular phenotypes were also investigated to probe the mechanisms underlying the resource allocation at a subcellular level. Overall, this work illustrates how yeast species optimize resource allocation among various compartments for metabolic reprogramming under fluctuating environments by combining the protein location annotation and large-scale absolute quantitative proteomics, thus providing a useful reference for establishing the direct connection between compartmentalization and cellular fitness.

Results

Reconstruction of a Unified Large-Scale Absolute Quantitative Proteome Dataset for Yeast. Proteome analysis has been widely employed to probe the metabolic activities of yeast, even though these datasets differ in the format and are stored in disparate locations for each study. To investigate how subcellular structure influenced protein resource allocation, we first collected all absolute quantitative yeast proteomics or relative ones from previous studies (5, 7, 9, 11–13, 15–17, 23–28). All collected relative proteomics were transformed into quantitative ones based on normalization and rescaling approaches (29, 30). Overall, 300 quantitative proteomes across nearly 150 distinct conditions were collected in this work mainly for two yeast species, *S. cerevisiae* and *I. orientalis.* Note that 275 of 300 proteomes were specific to *S. cerevisiae* and the rest to *I. orientalis*; hence, unless specifically mentioned, the analysis in this work was mainly based on datasets from *S. cerevisiae.*

The quality of yeast proteomics varied across datasets. For instance, the number of proteins detected by proteomics could range from 1,500 to 5,000 in the original datasets we gathered. To enhance the reliability of the compiled dataset, the high-quality proteomes with over 2,000 proteins detected in MS/MS were retained in priority (Fig. 1*A* and *SI Appendix*). Meanwhile, considering that the cell geometric information (i.e., cell size and surface area) was not known for parts of conditions, all types of protein abundance were transformed as mass fraction ($g/g_{total\ protein}$) for the subsequent comparative analysis (*SI Appendix*).

After quality analysis, we found that the yeast proteomes with unified mass fraction exhibited consistency, while some variances existed. To begin, the Pearson correlation coefficient (ρ) for any two samples was calculated, and it indicates that, in most cases, the ρ is over 0.5 (*SI Appendix*, Fig. S1*A*), showcasing a relatively good consistency in PMF between any two samples. In comparison, it displays that the quantity of detected proteins varied significantly between samples from different labs or studies (*SI Appendix*, Fig. S1*B*). In this regard, we examined the frequency of each protein detected in all samples and found some proteins were missing in nearly half of all samples (Fig. 1*B*). One major reason may be due to the fact that these proteins are in extreme low abundance within cells. Overall, it shows that the cumulative mass fraction of the 1,500 most frequently measured proteins in all samples is over 0.7 (Fig. 1*C*). It is also observed that, for each sample, the top 1,000 proteins with the highest abundance account for more than 90% of the mass of all measured proteins (*SI Appendix*, Fig. S1*C*), demonstrating that proteome analysis from each study accurately captured the majority of the cellular protein pool. With PMF, it is convenient to assess the profile of protein abundance across all conditions. For example, it clearly indicates that some proteins (e.g., YDL040C, YHR027C) have relatively lower abundance than other proteins (e.g., YBR127C, YHR064C), suggesting a consistent trend in protein expression across conditions (*SI Appendix*, Fig. S1*D*). However, when all proteins in each sample were evaluated, we found that the samples from the same studies tend to cluster together (*SI Appendix*, Fig. S1*E*). Such a phenomenon can be caused by a variety of factors, including but not limited to batch effects, variation in strains and experimental conditions, different amounts of detected proteins in each study, etc. As a result, it should be given careful consideration when conducting meta-analyses of proteome datasets collected from different studies or labs.

By comparison, our dataset is nearly twofold larger than those in previous studies (11, 31) in the size of absolute quantitative proteomics. With those curated proteome datasets in hand, an online database (https://yeast-proteome-database.streamlit.app/) was created, allowing for the investigation and visualization of PMF trends across conditions. For example, using the online database, the correlation of log-transformed mass fractions for any two samples could be calculated and the PMF distribution across different samples could be displayed based on user preferences (*SI Appendix*, Fig. S2). Thus, it is believed that this online database would be a useful resource for investigating the protein resource allocation across distinct growth environments. This online resource will be further expanded once additional yeast proteome datasets are available.

Given this heterogeneity in the compiled datasets, they were used in two distinct ways. First, the full collection of 300 proteomes spanning ~150 conditions was used to construct the database and

Downloaded from https://www.pnas.org by 155.4.17.34 on November 6, 2026 from IP address 155.4.17.34.

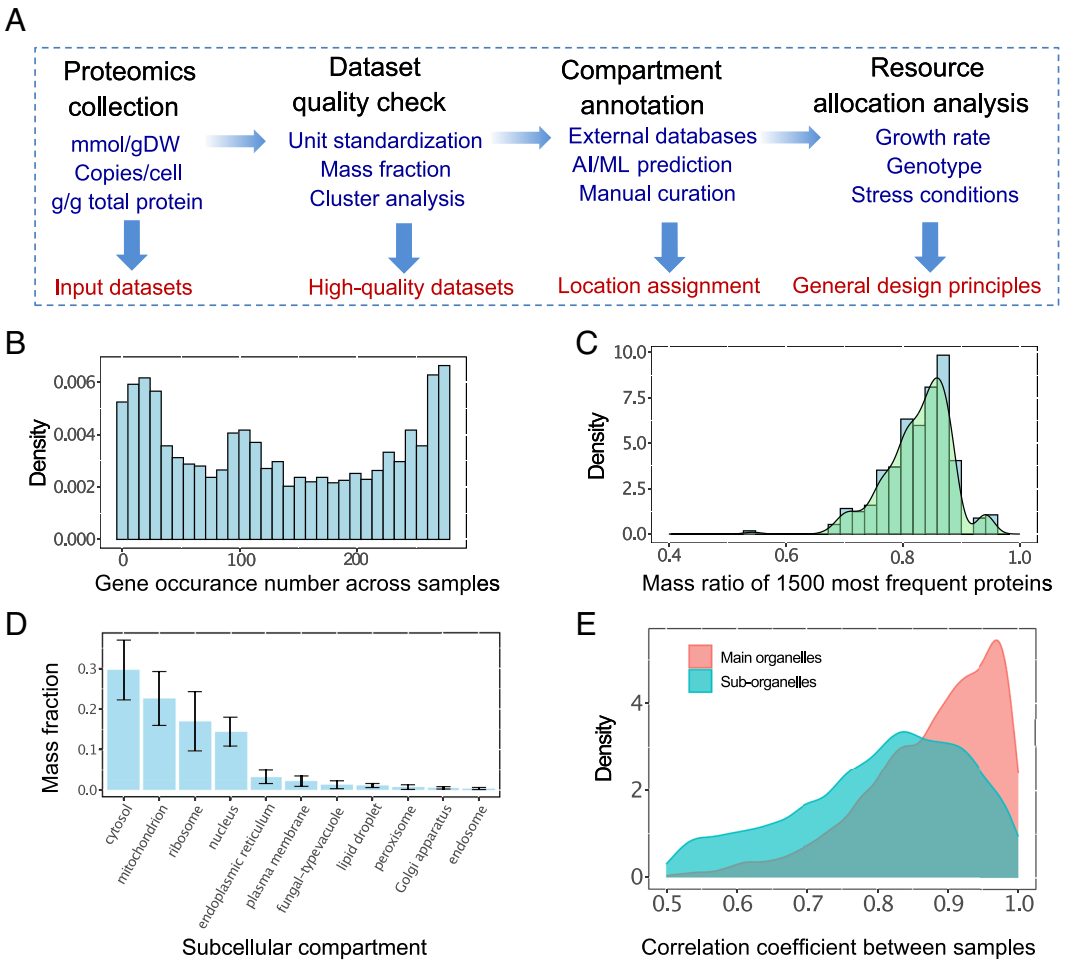


Fig. 1. Collection and quality analysis of proteomics datasets for yeast. The whole pipeline of this study from the yeast proteomics collection to the distillation of biological insights (*A*). Protein occurrence number analysis across all samples collected by this study (*B*). Statistical analysis of the mass fraction of 1,500 most frequently occurring proteins across samples (*C*). Conservation and variation in mass fraction for proteins from main subcellular compartments (*D*). Distribution of correlation coefficient calculated by PMF at compartment level across conditions (*E*).

to derive general patterns of protein distribution across subcellular compartments (Fig. 1 and *SI Appendix*, Figs. S1–S4). Second, a small number of carefully controlled datasets from specific studies were used to investigate physiology-dependent allocation of protein resources.

General Patterns of Resource Allocation at the Subcellular Compartment Level. Yeast possesses around 10 major subcellular compartments (32), each of which has a unique metabolic function within the cell. Some major compartments could be further divided into subcompartments. For example, as one single primary compartment (or organelle), mitochondria could be further divided into "Outer membrane," "Intermembrane space," "Inner membrane" and "Matrix." To examine how protein resources are allocated at (sub)compartment level, detailed cellular protein localization annotation was performed. First, all the protein annotations were retrieved from the SGD database, which was then carefully curated using some recent literature reports (*SI Appendix*). As a result, almost all *S. cerevisiae* proteins were assigned to one or more compartments (or subcompartments). For the latter, we calculated the mass fraction of proteins shared by two compartments per total protein mass using proteome data from batch conditions, and found that this mass fraction is smaller than 4% in most cases (*SI Appendix*, Fig. S3 *A* and *B*). As reported (10), some proteins could migrate dynamically into different compartments to execute the corresponding tasks in both compartments. To assess whether we can neglect these proteins in our analysis, we recalculated the mass fraction of proteins which could transfer across two compartments under different cell cycles from (10) and found that the number is smaller than 1% in most cases (*SI Appendix*, Fig. S3*C*), showcasing that this part of the proteome may not significantly influence our following analysis.

It is shown that the proteins were unevenly distributed among different compartments (*SI Appendix*, Fig. S4*A*). For example, some major compartments, e.g., nucleus and mitochondrion, contain over 1,000 proteins, while some smaller compartments, e.g., lipid droplet and P-body, only have less than 100 proteins. Compared to subcellular compartment annotation based on reliable experimental evidence, the number of proteins in some major compartments could be further refined (*SI Appendix*, Fig. S4*B*). Taking mitochondria and its subcompartments as examples, according to a recent work (33), the protein list in each component of mitochondria was updated. As a result, the number of total proteins in mitochondria decreased from 1,126 to 1,035, while the number of proteins in the mitochondrial inner membrane (MIM) decreased from 337 to 214 when compared to the protein annotation directly downloaded from the SGD database (34).

Combining PMF and protein locations, we computed the PMF for each compartment across ~150 unique conditions to explore the resource allocation at the compartment and subcompartment levels. As a whole, the protein resource is also unevenly distributed among different compartments. We found that, on average, the

Downloaded from https://www.pnas.org by 155.4.17.34 on November 6, 2026 from IP address 155.4.17.34.

cytosol has the highest percentage in mass fraction of protein resource (29.65 ± 7.40%), followed by the mitochondrion (22.61 ± 6.67%), ribosome (16.97 ± 7.33%), and nucleus (14.41 ± 3.57%). Note that the cytosol fraction represents nonribosomal cytoplasmic proteins. Except for the four major compartments, the mass fraction of protein for other major compartments was all smaller than 10% (Fig. 1*D*).

Next, our analysis revealed strikingly high correlations among PMFs of distinct compartments (or subcompartments) across all examined datasets (Fig. 1*E*). To further assess the general tendencies in protein resource allocation at the compartment level under different studies, the ρ in mass fraction at both the protein level and compartment level were computed between samples under batch cultivations. This comparison showed that the ρ ranged from 0.50 to 0.83 for protein-level mass fraction across studies, and from 0.92 to 0.99 for compartment-level mass fraction (*SI Appendix*, Fig. S4 *C* and *D*). Considering the lab-specific batch effects, we evaluated compartmental allocation trends separately within individual laboratory subsets (*SI Appendix*, Fig. S1 *F* and *G*). While baseline values shift slightly between labs, the general tendencies are reproducibly preserved. Thus, the relatively higher correlation at both the protein level and compartment level showcases the high quality of the proteome datasets we collected in this study.

Protein Resource Allocation at Compartment Level Correlates With Growth Rate. Previously, it was found that the proteome composition could covary with growth rate (the so-called growth law) (12, 35). Here, based on the unified PMF dataset spanning diverse conditions, we examined whether similar associations extend to resource allocation at the compartment and subcompartment scales. To this end, proteomics from carbon-limited chemostat cultivation was employed (5). First, we computed ρ between PMF from each component, including the major- and subcompartments, according to the proteomics under a series of growth rates from carbon-limited chemostat cultivation. We found there exists a positive correlation between PMFs for some subcellular components (e.g., ribosome and mitochondria inner membrane) and growth under carbon-limited condition (*SI Appendix*, Fig. S5*A*). Meanwhile, the negative correlation between PMF and growth was also observed for lots of compartments, e.g., vacuole and lipid droplet. It initially indicates that there exists a trade-off in protein resource allocation at the compartment level along with cellular growth. At the major compartment level, we found that the mass fraction of ribosome increased consistently with growth rate under both nitrogen- and carbon-limited chemostat cultivations (Fig. 2*A* and *SI Appendix*, Fig. S6), while the mass fraction of proteins from other major compartments mostly decreased along with growth rate. It may be because the cell needs to redistribute more resources into the protein synthesis machinery from other major compartments to meet the high demand for growth.

Interestingly, if checking the resource allocation at the subcompartment level from the nucleus, we found that the PMF of the nucleolus increases linearly with the cellular growth rate, although the PMF of the nucleus shows the opposite trend (*SI Appendix*, Figs. S5B and S6). Such a phenomenon may be due to the fact that the nucleolus within the nucleus is responsible for producing and assembling ribosomes. Thus, the higher demand in ribosome will correspondingly promote the increase in the PMF of the nucleolus. On the contrary, it shows that PMF of nuclear periphery decreased consistently as growth rate increased, showcasing the trade-off in resource allocation within nucleus. At a lower specific growth rate, the higher PMF of the nuclear periphery may represent a reserve of proteins, which is similar to the reserve of enzymes from metabolic superpathways (13). It is speculated that as the PMF of the nucleus decreased at higher specific growth rates, the resource within the nucleus may be reallocated to maintain the normal function of the nucleus. Whether individual proteins also physically relocate between these subcompartments cannot be resolved by our approach and would require localization-resolved experimental measurements.

The similar trade-off in resource allocations was also found for mitochondria, one key major organelle of eukaryal cells (*SI Appendix*, Fig. S5*C*). We found the PMFs of four subcompartments from mitochondria, including MIM and mitochondrial matrix, first increased with specific growth rate before the critical point and then decreased accordingly. It is well known that *S. cerevisiae* has metabolic overflow under high specific growth rates with glucose as the substrate. It is reported that once overflow started, more protein resources were channeled into the fermentation pathway from the respiration pathway (15). Here, our result initially illustrates the tendencies in resource allocation at the compartment level, as well as at the subcompartment level of mitochondria, related to the occurrence of overflow.

It is observed that a part of the proteins could be located in multiple compartments within a cell. Does the compartment itself really impose constraints on resource allocation? Here, to answer this question, we randomly selected hundreds of proteins (e.g., 200, 500, and 1,000) 1,000 times, the number of which is in the range of the protein number within each major compartment, and then checked the correlation between the PMFs of those randomly selected proteins and specific growth rate. Clearly, it shows that if the proteins were randomly selected, not considering the protein location, there is no correlation between the PMF of sampled proteins and the specific growth rate, therefore indicating that resource allocation is closely tied to subcellular compartment identity rather than occurring at random (*SI Appendix*, Fig. S7).

Metabolic Shift Induced by Nutrient Limitation Results in Protein Resource Allocation at Compartment Level. Yeast always encounters resource deficiencies in the environment, which may be accompanied with a metabolic shift to optimize resource utilization. It is known that nitrogen limitation could influence the cellular metabolism significantly. It is unclear how cellular protein resources are reallocated under different levels of nitrogen limitation. To alleviate the effects of regulation by growth rates, the proteomic dataset under different C/N ratios with growth rate controlled at 0.2 h^{-1} using chemostat cultivation was reanalyzed in this study (13). In general, we found that the protein resource allocation at the compartment level exhibited high robustness, as the adjusted R^2 between PMFs of compartments from different C/N ratios is over 0.90, though it is slightly decreased from 0.962 at C/N = 30 to 0.928 at C/N = 115 (Fig. 2*B*). With the intensification of nitrogen resource limitation, we also found that the PMF of the ribosome decreased slightly. Note that the specific growth rate under different C/N ratios was kept at 0.2 h^{-1}, thus maybe some nonessential proteins from the ribosome were more degraded to meet the protein demand in other compartments. Interestingly, it is found that the PMF within vacuole was increased, which may accelerate the resource recycling under extreme N limitation (*SI Appendix*, Fig. S8*A*).

As another example, yeast could stop normal growth under serious zinc deficiency, thus providing chances to probe the resource allocation related to extreme nutrient limitation. In this aspect, the PMFs of compartments were recalculated using proteomics sampled at 0 h, 4 h, 8 h, and 12 h after the onset of zinc deficiency (24). Overall, PMFs of compartments at different time

Downloaded from https://www.pnas.org by 155.4.17.34 on November 6, 2026 from IP address 155.4.17.34.

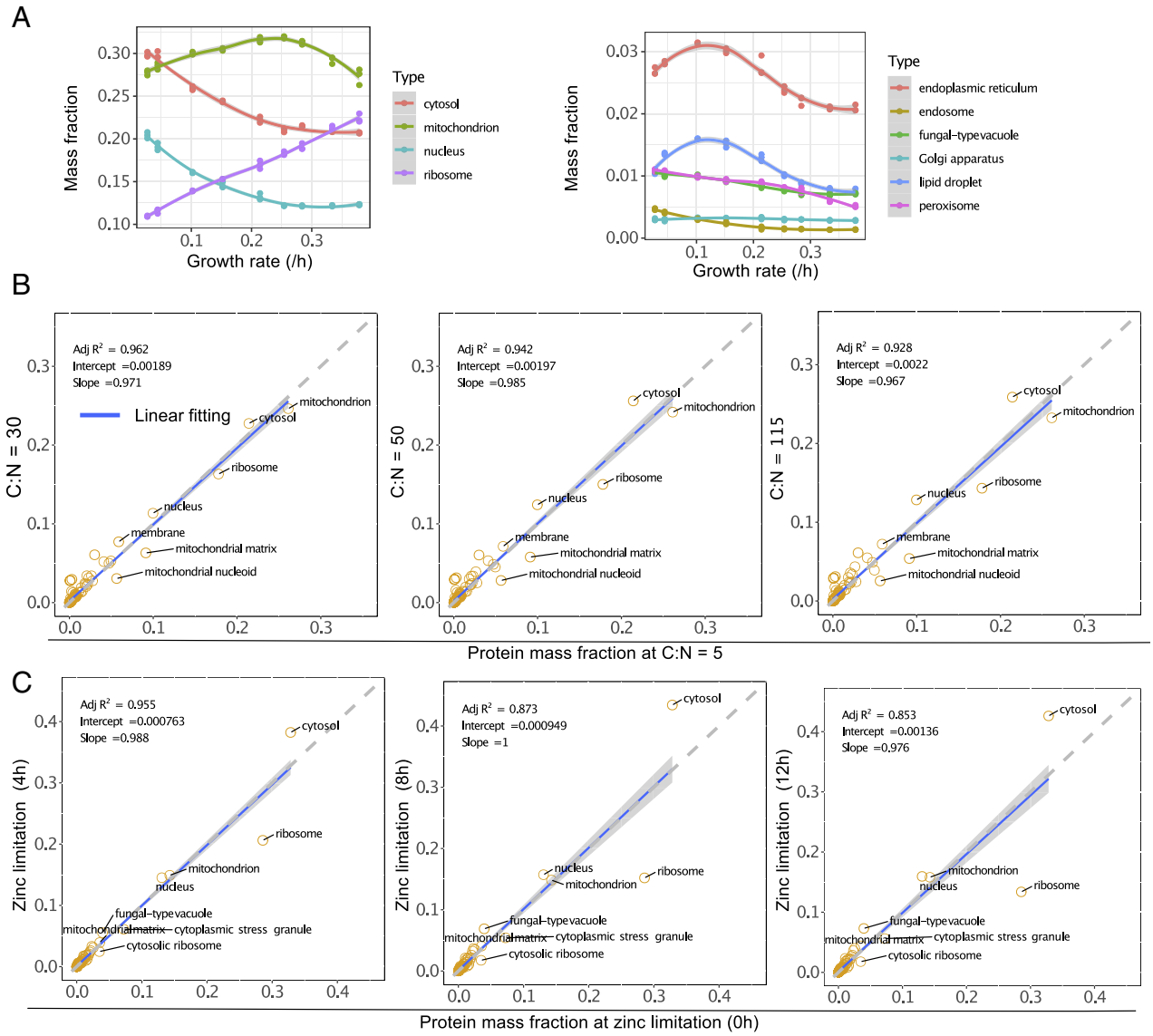


Fig. 2. Growth rate and nutrient limitation significantly regulate protein resource redistribution at subcellular compartment level. Detailed correlation between the main compartment's PMF and the growth rate under carbon-limited chemostat cultivation (*A*). Reallocation of compartmental PMFs under chemostat cultivation with varying nitrogen limitation levels (C:N ratios = 30, 50, 115) compared to that at C:N = 5 under a constant growth rate ($\mu = 0.2\ h^{-1}$) (*B*). Reallocation of compartmental PMFs at 4 h, 8 h, and 12 h, compared to that at the start (0 h) of zinc deficiency (*C*).

points were highly correlated (Fig. 2*C*, adjusted $R^2 > 0.853$). By comparison, as the extent of starvation increased, PMFs of compartments deviated more from those at 0 h. For example, using the linear fitting, the adjusted R^2 at 12 h is decreased to 0.853 compared to 0.955 at 0 h. When looking into the deviation at the compartment level, it shows that lots of compartments' PMF at 4 h, 8 h, 12 h were significantly different from that at 0 h, indicating the cell reallocates protein resources to respond to the zinc deficiency. Specifically, we found that along with the zinc deficiency, the PMF of the ribosome decreased while the PMF of the mitochondria and cytosol increased, showing that protein used for anabolism was reduced. Interestingly, it is noted that the PMFs of the lipid droplet and vacuole are increased accordingly, which is similar to the above nitrogen limitation (*SI Appendix*, Fig. S8*B*). With zinc deficiency, the cellular resource would become limited, and the higher PMF within vacuole may be related to enhanced catabolic activities within the cell, which could, to some extent, contribute to resource recycling and maintain normal cellular function.

Overall, these results suggest that protein resources were relocated in a similar pattern under N limitation and zinc deficiency, and cells would resist the nutrient limitation by resource allocation at the compartment level as a whole.

Quantitative Correlations Between Protein Abundance, Compartment-Level Resource Distribution, and Cellular Phenotypes. The aforementioned analysis indicates that there exists a direct correlation between PMFs of compartments and cellular physiological parameters. Here we thoroughly explored how PMFs from major compartments together could play a significant role in determining the cellular traits, not only specific growth rate, but also the specific uptake rates of glucose ($q_{glucose}$) and oxygen (q_{O2}) as well as the specific carbon dioxide production rate (q_{CO2}). We first fitted the formulas using a larger proteomics dataset acquired under nitrogen-limited chemostat condition with diverse nitrogen sources (5) and then tested the formulas using an independent carbon-limited chemostat dataset (12) (Fig. 3 *A* and *B* and *SI Appendix*). Overall, we found that the

Downloaded from https://www.pnas.org by 155.4.17.34 on November 6, 2026 from IP address 155.4.17.34.

linear combinations of PMFs from 2 to 3 key compartments are sufficient to achieve high predictive accuracy for most phenotypes (*SI Appendix*, Fig. S9*A*). Notably, the specific growth rate is better predicted by a combination of ribosomal, nucleolar, and plasma membrane PMFs than by ribosomal PMF alone. Although it has been reported that the growth rate is linearly correlated with the PMF of the ribosome (26), we found that the formula based on the aforementioned three compartments performs better across two independent datasets (*SI Appendix*, Fig. S9*B*). For $q_{glucose}$ and q_{CO2}, the PMFs of ribosome and nucleus could predict them better than only using one of them. Meanwhile, for q_{O2}, the PMFs of ribosome and mitochondrial inner membrane could also enhance the prediction performance. Overall, it may suggest that there exist some potential correlations between compartment-level resource allocation and the global cellular physiology.

Thus, changes in PMFs from several key compartments could, to a large extent, determine growth-related parameters of yeast, but what is the mechanism underlying the resource reallocation among different compartments? Can we find a group of proteins to predict the general resource allocation at the subcellular compartment level? To evaluate this, we built a model linking the PMF of all proteins to the PMF of seven major compartments (mitochondrion, nucleus, endoplasmic reticulum, fungal-type vacuole, plasma membrane, ribosome, and cytosol), using linear ridge regression coupled with

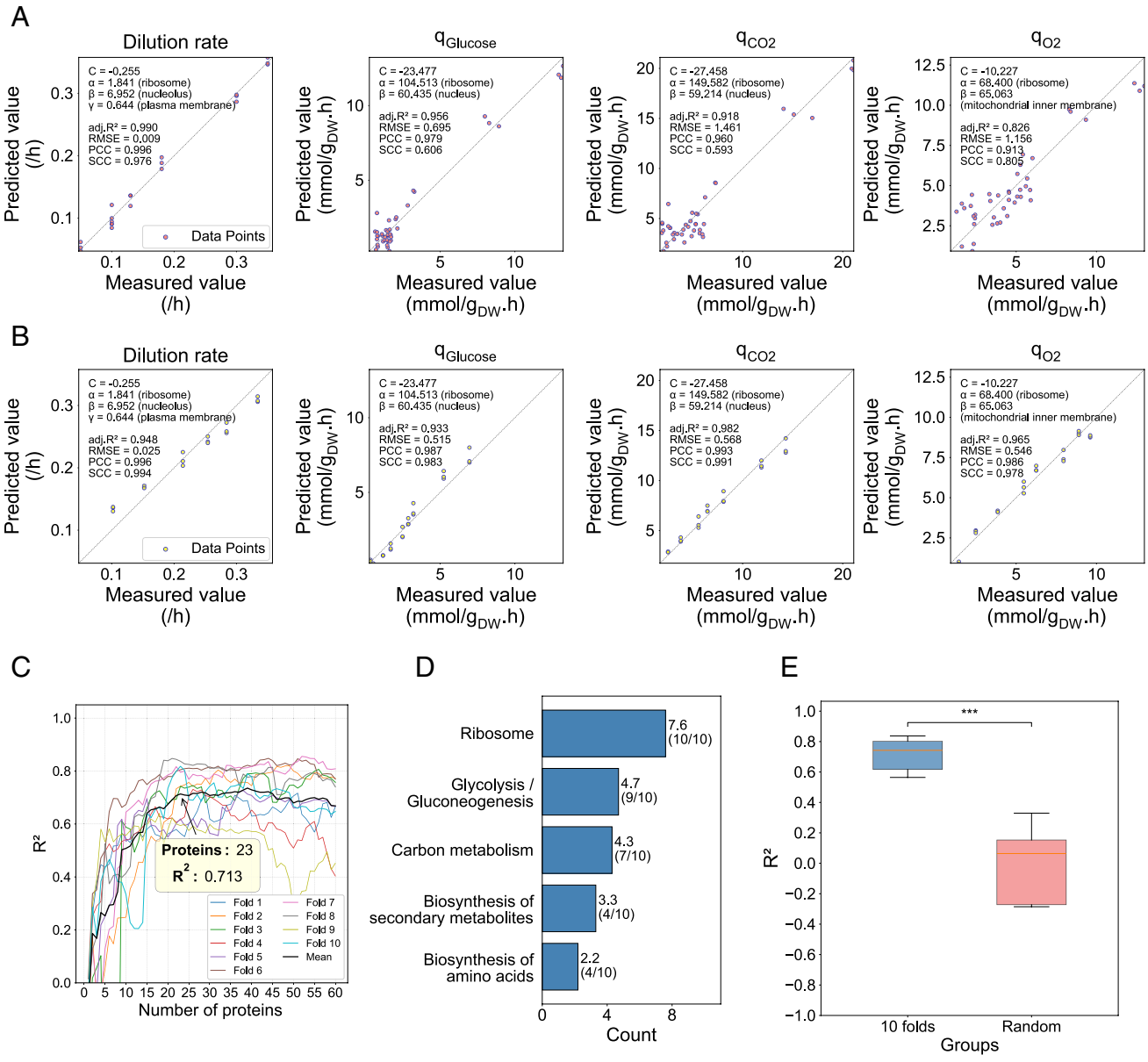


Fig. 3. Quantitative correlations between protein abundance, compartment-level resource distribution, and cellular phenotypes. Fitting of the linear correlations between the PMFs of compartments/subcompartment and yeast physiological parameters using Yu's large-scale dataset to obtain the formulas (*A*). Validation of the above formulas using Xia's dataset (*B*). Relationship between the number of selected proteins and test-set R^2 for ridge regression models predicting compartment-level resource allocation. Features were selected using 10-fold Recursive Feature Elimination (RFE), i.e., the training/validation data were split into 10-folds (partitions), with each colored line ("Fold 1"–"Fold 10") showing the result of leaving that partition out for validation while training on the remaining nine; the bold black line is the mean across the 10-folds. For each fold, the best-performing model was chosen from candidate feature counts ranging from 1 to 60, yielding an optimal size of 23 proteins (*C*). Top 5 terms from KEGG pathway enrichment (adjusted *P* value < 0.05) across 10-folds, ranked by average gene count. Enrichment was performed separately for the 23 proteins selected in each fold, then results were aggregated. Bars show the average gene count per fold, and labels indicate the mean count and the number of folds in which the term was enriched (n/10) (*D*). Comparison of R^2 on the independent test set for two feature-selection strategies: 10-folds (fold-specific 23-protein sets selected by 10-fold RFE), and Random (10 randomly sampled 23-protein sets). ***P value < 0.001 (*E*).

Downloaded from https://www.pnas.org by 155.4.17.34 on November 6, 2026 from IP address 155.4.17.34.

10-fold RFE (*SI Appendix*, Fig. S10). We found that a minimal set of 23 proteins could capture the resource allocation across seven major compartments (average test-set R^2 = 0.713, Fig. 3*C* and Dataset S1). When removing the selected 23 proteins from the seven major compartments, there still exist correlations between the remaining mass fraction of these compartments and the PMFs of these 23 proteins (average test-set R^2 = 0.654, *SI Appendix*, Fig. S10). We next evaluated the evolutionary conservation of these proteins based on previous studies (36–38). Across *S. cerevisiae* strains, the RFE-selected 23 proteins exhibit significantly lower sequence divergence (dN/dS) than size-matched randomly selected proteins (*SI Appendix*, Fig. S11), indicating strong purifying selection. Their expression levels also show lower divergence across strains, and their protein half-lives are longer than those of the random sets, consistent with the well-documented stability of ribosomal proteins and core metabolic enzymes (38, 39). Further, KEGG enrichment analysis revealed that these selected proteins are predominantly involved in core metabolic processes, including the ribosome (adjusted *P* value < 0.05), glycolysis/gluconeogenesis (adjusted *P* value < 0.001), and carbon metabolism (adjusted *P* value < 0.05) (Fig. 3*D* and *SI Appendix*, Fig. S10). Similarly, we performed Gene Ontology (GO) enrichment analysis on the selected protein set. The GO terms most consistently enriched in the Biological Process category were generation of precursor metabolites and energy (adjusted *P* value < 0.001) together with cytoplasmic translation and related central-carbon processes (adjusted *P* value < 0.01), in agreement with the KEGG results. Additionally, protein–protein interaction (PPI) network analysis (*SI Appendix*, Fig. S12) showed that this protein set is highly interconnected, with an average node degree of 7.30 and a local clustering coefficient of 0.67, significantly higher than those of randomly selected protein sets. Importantly, the protein sets found by RFE performed significantly better than randomly selected protein sets in reflecting subcellular resource allocation across the seven major compartments (Fig. 3*E*). Together, these results suggest that there exists a potential correlation between the abundance of a minimal protein set and the global cellular resource allocation across seven major compartments.

Subcellular Compartment-Level Resource Allocation Varied Between Two Distinct Yeast Species. Last, we further asked whether protein resource allocation could be comparable between yeast species with distinct physiological traits and evolutionary backgrounds. Here, using *I. orientalis*—a Crabtree-negative yeast species—as a typical example, we compared the PMFs of compartments between *S. cerevisiae* CEN.PK (Crabtree-positive) and *I. orientalis* SD108 (Crabtree-negative) under various growth conditions using a series of high-quality proteomic datasets generated by a recent study (16).

To probe the resource allocation at subcellular compartment levels in *I. orientalis*, we first assigned compartment information to each protein from *I. orientalis* (*SI Appendix*). Even with different procedures in protein location annotation, the numbers of proteins from different compartments follow a similar pattern to that of *S. cerevisiae*, with the nucleus having the most proteins, followed by mitochondria (*SI Appendix*, Fig. S13*A*). Three annotation procedures were utilized, and the number of proteins identified by ortholog relation is largest (*SI Appendix*, Fig. S13*B*). Once the protein location was annotated, the PMFs of compartments for *I. orientalis*, as well as the ρ of PMFs across samples, were calculated under batch, carbon-limited, nitrogen-limited, and phosphorus-limited growth conditions. In general, the resource allocation at the compartment level from *I. orientalis* showed substantial similarity to patterns in *S. cerevisiae* (*SI Appendix*, Fig. S13 *C* and *D*), lending evidence for the protein localization annotation for *I. orientalis* used in this work. By contrast, it is found that the PMF of mitochondrion is higher than that of cytosol within *I. orientalis*, which may be because Crabtree-negative yeasts invest more resources in mitochondria to improve energy supply efficiency (16).

Next, the PMFs of compartments under anaerobic conditions and respiration inhibition were compared to those under normal aerobic conditions for *S. cerevisiae* and *I. orientalis*, respectively. At first glance, we found that these perturbations more significantly affect protein resource allocation at the compartment level in *I. orientalis* than in *S. cerevisiae*, partially consistent with prior observations (16, 40). As shown in Fig. 4 *A* and *B*, it seems that protein resource allocation in *S. cerevisiae* remains relatively stable under these conditions. In contrast, *I. orientalis* exhibits pronounced redistribution of protein resources. Specifically, it could be found that the PMFs of the mitochondria and cytosol increase in *I. orientalis,* while the PMFs of the ribosome decrease under the above two conditions, likely reflecting the stronger growth impairment when respiration is repressed in this species.

Further, we compared the PMFs of compartments for both yeast species under a series of different conditions and performed cluster analysis of samples based on these PMFs (Fig. 4 *C* and *D*). For both yeast species, batch cultivation could be distinguished from chemostat cultivations under various nutrient (C/N/P) limitations. More importantly, unlike *S. cerevisiae,* cultivation of *I. orientalis* under O_2 deprivation or respiration inhibition can be clearly distinguished from other conditions where the O_2 is sufficient or the respiration is uninhibited. Although these quantitative differences are consistent with the known physiological divergence between the two yeast species, we note that *S. cerevisiae* and *I. orientalis* differ in several important respects beyond their Crabtree status, including their whole-genome duplication history, domestication background, and ecological niche. Consequently, we present our results as compartment-scale evidence that is consistent with a general resource allocation difference between Crabtree-positive and Crabtree-negative yeasts, rather than as definitive proof. Testing additional species pairs across independent Crabtree-positive and Crabtree-negative lineages will be necessary to confirm whether the pattern observed here is broadly generalizable.

Discussion

This study systematically explores how limited protein resource is reallocated among subcellular compartments within yeast cells under a wide range of conditions through leveraging the largest absolute quantitative proteome dataset (300 proteomes spanning ~150 conditions) for two yeast species, *S. cerevisiae* and *I. orientalis*. In general, the compartment-level protein resource allocation was significantly affected by cell growth rate, nutrient limitation, and genomic background. More importantly, our integrated analysis shows that there exist close correlations between protein abundance, compartment-level resource allocation, and cellular physiological parameters. It suggests that the PMFs from a limited number of compartments could be correlated to the cellular physiological parameters while a limited number of proteins could track the variation in the general resource allocation at the subcellular compartment level. It may suggest that the compartment-level resource redistribution was precisely tuned for cellular metabolic adaption at different scales.

Crucially, these quantitative principles could provide additional constraints for cellular metabolic models to guide the metabolic

Downloaded from https://www.pnas.org by 155.4.17.34 on November 6, 2026 from IP address 155.4.17.34.

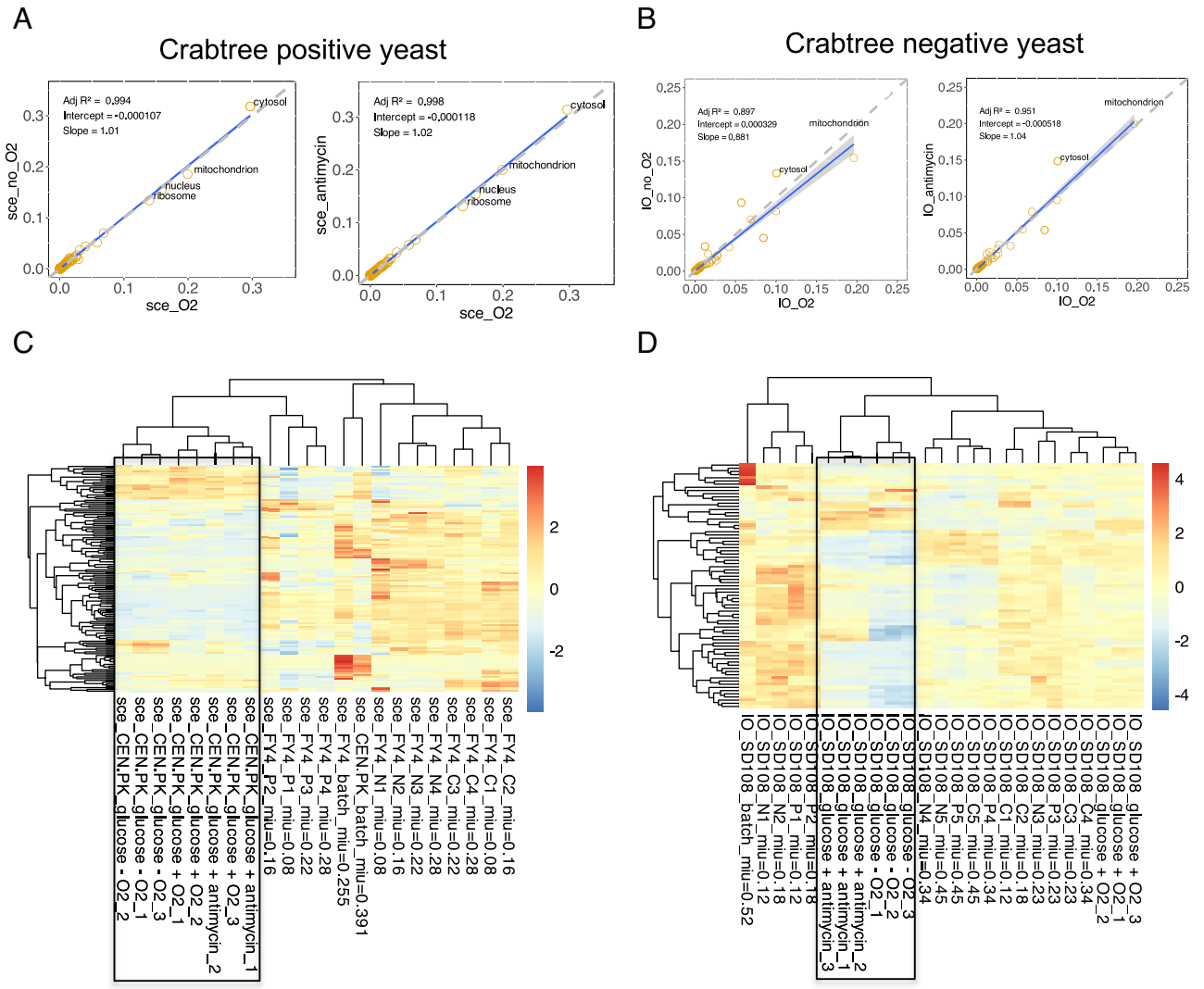


Fig. 4. Comparison of resource allocation among subcellular compartments for two different yeast species—*S. cerevisiae* (sce, Crabtree-positive) *and I. orientalis* (IO, Crabtree-negative) under different conditions. Influence of the anaerobic and antimycin-inhibited condition on protein resource redistribution at compartment level for Crabtree positive and negative yeasts (*A* and *B*). Heatmap of mass fraction at compartment level across different conditions from the same study with cluster analysis of different samples for Crabtree positive and negative yeasts, in which the samples under anaerobic and antimycin-inhibited conditions from IO could be clearly separated from other conditions (*C* and *D*). Each row of heatmap represents a component.

engineering. For example, the compartment-level resource allocation could be used to improve the prediction performance of enzyme constrained metabolic models (ecGEMs) during in silico cell factory design for products with high protein costs (41). Furthermore, by delineating compartment-specific resource allocation and proteomic redundancy across diverse growth phases, our work offers potential clues for rational design of chassis strains, in which the protein resources could be precisely reallocated from nonessential compartmental functions to heterologous pathways, thereby optimizing the metabolic trade-off between cellular fitness and bioproductivity (42).

Our meta-analysis in yeast proteomics still faces several significant challenges, including batch effects and data heterogeneity, among which the variations in strain/species backgrounds, growth environments, and limit of detection by mass spectrometry further complicate cross-study comparisons, especially for low-abundance proteins. It is observed that different derived strains of *S. cerevisiae*, such as S288C and CEN.PK, exhibit distinct metabolic profiles and physiological characteristics (40), thus the subcellular protein resource allocation may be strain-dependent. Note that the protein localization annotation used in this work was mainly based on existing databases or computational inferences and thus fails to capture dynamic relocalization of functional proteins under dynamic conditions (10), such as stress-induced protein migration between compartments (43). Additionally, the limitation in protein localization annotation at the suborganelle level makes it impossible to conduct accurate resource allocation analysis at a higher resolution. Consequently, the initial correlations (e.g., the correlation between 23 proteins' abundance and PMFs of seven major compartments) inferred in this work should be further evaluated when new independent proteomes are released. Caution should therefore be taken if some of the conclusions of this study are extrapolated to data from other conditions out of this work. By addressing these challenges, future studies can reveal a more dynamic, high-resolution picture describing the resource allocation at multiscale levels from major subcellular compartments to single proteins, which will help to profile the function of various compartments related to cellular fitness (44).

In summary, the unified large-scale absolute quantitative proteomic dataset, along with the online database, will serve as a valuable resource for yeast systems biology studies, enabling

Downloaded from https://www.pnas.org by 155.4.17.34 on November 6, 2026 from IP address 155.4.17.34.

the exploration of the protein resource allocation at the compartment level under a wide range of varied growth conditions. By linking compartment-scale proteomics to cell physiology, metabolism, and evolution, this work sheds light on the principles in resource allocation for eukarya, setting a solid foundation to bridge the gaps between compartment functions and cellular metabolic adaptation.

Methods and Materials

All the materials and methods are detailed in *SI Appendix*: proteomic dataset collection; proteome quality filtering to exclude low-coverage datasets (< 1500 proteins detected in some cases); protein subcellular localization; formula fitting between compartments' PMF and yeast physiological parameters; RFE with ridge regression to identify a minimal protein set in prediction of compartment-level resource allocation; PPI network analysis; and quantification and statistical analysis.

Data, Materials, and Software Availability. The unified yeast proteomic dataset can be found at https://yeast-proteome-database.streamlit.app and https://github.com/hongzhonglu/large_scale_yeast_proteomics_analysis (45). All Study data are included in the article and/or supporting information.

ACKNOWLEDGMENTS. This work is supported by Grant 2022YFA0913000 from the National Key R&D Program of China, Grants 22208211 and 22378263 from the National Natural Science Foundation of China. We thank Hao Yu and Xueting Wang for help in the data analysis.

Author affiliations: [a]State Key Laboratory of Microbial Metabolism, School of Life Science and Biotechnology, Shanghai Jiao Tong University, Shanghai 200240, China; [b]Institute of Natural Sciences, School of Mathematical Sciences, Zhangjiang Institute of Advanced Study, Shanghai Jiao Tong University, Shanghai 200240, China; [c]Shanghai AI Laboratory, Shanghai 200232, China; [d]BioInnovation Institute, Ole Måløes Vej, Copenhagen N DK2200, Denmark; and [e]Department of Life Sciences, Chalmers University of Technology, Gothenburg SE412 96, Sweden

Author contributions: H.L. and J.N. designed research; H.L. and S.H. performed research; Y.Z. and Y.W. contributed new reagents/analytic tools; Z.Z. and F.T. analyzed data; and H.L. and J.N. wrote the paper.

1. J. M. Archibald, Endosymbiosis and eukaryotic cell evolution. *Curr. Biol.* **25**, R911–R921 (2015).
2. L. Bar-Peled, N. Kory, Principles and functions of metabolic compartmentalization. *Nat. Metab.* **4**, 1232–1244 (2022).
3. S. K. Hammer, J. L. Avalos, Harnessing yeast organelles for metabolic engineering. *Nat. Chem. Biol.* **13**, 823–832 (2017).
4. T. Xu, Q. Wang, Q. Wang, L. Sun, Mass spectrometry-intensive top-down proteomics: An update on technology advancements and biomedical applications. *Anal. Methods-UK* **16**, 4664–4682 (2024).
5. R. Yu, E. Vorontsov, C. Sihlbom, J. Nielsen, Quantifying absolute gene expression profiles reveals distinct regulation of central carbon metabolism genes in yeast. *eLife* **10**, e65722 (2021).
6. I. T. Kleijn *et al.*, Growth-rate-dependent and nutrient-specific gene expression resource allocation in fission yeast. *Life Sci. Alliance* **5**, e202101223 (2022).
7. F. Di Bartolomeo *et al.*, Absolute yeast mitochondrial proteome quantification reveals trade-off between biosynthesis and energy generation during diauxic shift. *Proc. Natl. Acad. Sci. U.S.A.* **117**, 7524–7535 (2020).
8. C. B. Messner *et al.*, The proteomic landscape of genome-wide genetic perturbations. *Cell* **186**, 2018–2034.e2021 (2023).
9. K. Campbell *et al.*, Building blocks are synthesized on demand during the yeast cell cycle. *Proc. Natl. Acad. Sci. U.S.A.* **117**, 7575–7583 (2020).
10. A. Litsios *et al.*, Proteome-scale movements and compartment connectivity during the eukaryotic cell cycle. *Cell* **187**, 1490–1507.e1421 (2024).
11. B. Ho, A. Baryshnikova, G. W. Brown, Unification of protein abundance datasets yields a quantitative *Saccharomyces cerevisiae* proteome. *Cell Syst.* **6**, 192–205.e3 (2018).
12. J. Xia *et al.*, Proteome allocations change linearly with the specific growth rate of *Saccharomyces cerevisiae* under glucose limitation. *Nat. Commun.* **13**, 2819 (2022).
13. R. Yu *et al.*, Nitrogen limitation reveals large reserves in metabolic and translational capacities of yeast. *Nat. Commun.* **11**, 1881 (2020).
14. E. Metzl-Raz *et al.*, Principles of cellular resource allocation revealed by condition-dependent proteome profiling. *eLife* **6**, e28034 (2017).
15. C. Malina, R. Yu, J. Bjorkeroth, E. J. Kerkhoven, J. Nielsen, Adaptations in metabolism and protein translation give rise to the Crabtree effect in yeast. *Proc. Natl. Acad. Sci. U.S.A.* **118**, e2112836118 (2021).
16. Y. Shen *et al.*, Mitochondrial ATP generation is more proteome efficient than glycolysis. *Nat. Chem. Biol.* **20**, 1123–1132 (2024).
17. P. J. Lahtvee *et al.*, Absolute quantification of protein and mRNA abundances demonstrate variability in gene-specific translation efficiency in yeast. *Cell Syst.* **4**, 495–504 (2017).
18. W.-K. Huh *et al.*, Global analysis of protein localization in budding yeast. *Nature* **425**, 686–691 (2003).
19. M. Y. Hein *et al.*, Global organelle profiling reveals subcellular localization and remodeling at proteome scale. *Cell* **188**, 1137–1155 e1120 (2025).
20. E. Wiederhold, L. M. Veenhoff, B. Poolman, D. J. Slotboom, Proteomics of *Saccharomyces cerevisiae* organelles. *Mol. Cell. Proteomics* **9**, 431–445 (2010).
21. Y. Kurikawa, I. Koyama-Honda, N. Tamura, S. Koike, N. Mizushima, Organelle landscape analysis using a multiparametric particle-based method. *PLoS Biol.* **22**, e3002777 (2024).
22. D. J. Nightingale, A. Geladaki, L. M. Breckels, S. G. Oliver, K. S. Lilley, The subcellular organisation of *Saccharomyces cerevisiae*. *Curr. Opin. Chem. Biol.* **48**, 86–95 (2019).
23. I. E. Elsemman *et al.*, Whole-cell modeling in yeast predicts compartment-specific proteome constraints that drive metabolic strategies. *Nat. Commun.* **13**, 801 (2022).
24. Y. Wang *et al.*, The cellular economy of the Saccharomyces cerevisiae zinc proteome. *Metallomics* **10**, 1755–1776 (2018).
25. N. A. Kulak, G. Pichler, I. Paron, N. Nagaraj, M. Mann, Minimal, encapsulated proteomic-sample processing applied to copy-number estimation in eukaryotic cells. *Nat. Methods* **11**, 319–324 (2014).
26. J. Björkeroth *et al.*, Proteome reallocation from amino acid biosynthesis to ribosomes enables yeast to grow faster in rich media. *Proc. Natl. Acad. Sci. U.S.A.* **117**, 21804–21812 (2020).
27. R. Kumar, P.-J. Lahtvee, Proteome overabundance enables respiration but limitation onsets carbon overflow. bioRxiv [Preprint] (2020). https://doi.org/10.1101/2020.02.20.957662 (Accessed 20 February 2020).
28. F. Li *et al.*, Deep learning-based kcat prediction enables improved enzyme-constrained model reconstruction. *Nat. Catal.* **5**, 662–672 (2022).
29. B. J. Sanchez *et al.*, Benchmarking accuracy and precision of intensity-based absolute quantification of protein abundances in Saccharomyces cerevisiae. *Proteomics* **21**, e2000093 (2021).
30. A. Millan-Oropeza, M. Blein-Nicolas, V. Monnet, M. Zivy, C. Henry, Comparison of different label-free techniques for the semi-absolute quantification of protein abundance. *Proteomes* **10**, 2 (2022).
31. M. Wang *et al.*, PaxDb, a database of protein abundance averages across all three domains of life. *Mol. Cell. Proteomics* **11**, 492–500 (2012).
32. J. Zhu *et al.*, A validated set of fluorescent-protein-based markers for major organelles in yeast (*Saccharomyces cerevisiae*). *mBio* **10**, e01691–19 (2019).
33. M. Morgenstern *et al.*, Definition of a high-confidence mitochondrial proteome at quantitative scale. *Cell Rep.* **19**, 2836–2852 (2017).
34. J. M. Cherry *et al.*, *Saccharomyces* genome database: The genomics resource of budding yeast. *Nucleic Acids Res.* **40**, D700–D705 (2012).
35. S. Hui *et al.*, Quantitative proteomic analysis reveals a simple strategy of global resource allocation in bacteria. *Mol. Syst. Biol.* **11**, 784 (2015).
36. J. Peter *et al.*, Genome evolution across 1, 011 *Saccharomyces cerevisiae* isolates. *Nature* **556**, 339–344 (2018).
37. É. Caudal *et al.*, Pan-transcriptome reveals a large accessory genome contribution to gene expression variation in yeast. *Nat. Genet.* **56**, 1278–1287 (2024).
38. R. Christiano, N. Nagaraj, F. Frohlich, T. C. Walther, Global proteome turnover analyses of the yeasts *S. cerevisiae* and *S. pombe*. *Cell Rep.* **9**, 1959–1965 (2014).
39. A. Belle, A. Tanay, L. Bitincka, R. Shamir, E. K. O'Shea, Quantification of protein half-lives in the budding yeast proteome. *Proc. Natl. Acad. Sci. U.S.A.* **103**, 13004–13009 (2006).
40. A. B. Canelas *et al.*, Integrated multilaboratory systems biology reveals differences in protein metabolism between two reference yeast strains. *Nat. Commun.* **1**, 145 (2010).
41. H. Wang *et al.*, Resource-aware cell factory design through multi-scale metabolic models with expression and proteome constraints. *Fundamental Res.* (2026). 10.1016/j.fmre.2026.07.008.
42. J. Mao *et al.*, Relieving metabolic burden to improve robustness and bioproduction by industrial microorganisms. *Biotech. Adv.* **74**, 108401 (2024).
43. A. Platzek, K. Odehnalová, J. P. Schessner, G. H. H. Borner, S. Schuck, Dynamic organellar mapping in yeast reveals extensive protein localization changes during ER stress. *Nat. Commun.* **16**, 10842 (2025).
44. S. Peng, B. Li-zhe, C. Hong, L. Dan, Stress response of membrane-based cell organelles in budding yeast. bioRxiv [Preprint] (2024). https://doi.org/10.1101/2024.09.08.611912 (Accessed 8 September 2024).
45. H. Lu, hongzhonglu/large_scale_yeast_proteomics_analysis: v 1.0.2 yeast_proteomics. Zenodo. https://doi.org/10.5281/zenodo.23299111. Accessed 11 October 2026.

Downloaded from https://www.pnas.org by 155.4.17.34 on November 6, 2026 from IP address 155.4.17.34.